Hindawi Publishing Corporation
International Journal of Rotating Machinery
Volume 2009, Article ID 349397, 7 pages
doi:10.1155/2009/349397

Research Article

Numerical Estimation of Torsional Dynamic Coefficients of a Hydraulic Turbine

Martin Karlsson,[1] Håkan Nilsson,[2] and Jan-Olov Aidanpää[3]

[1] *Lloyd's Register ODS, 10074 Stockholm, Sweden*
[2] *Department of Fluid Dynamics, Chalmers University of Technology, 41296 Göteborg, Sweden*
[3] *Division of Solid Mechanics, Department of Mechanical Engineering, Luleå University of Technology, 97187 Luleå, Sweden*

Correspondence should be addressed to Martin Karlsson, martin.karlsson@lr-ods.com

Received 2 November 2008; Revised 4 March 2009; Accepted 2 April 2009

Recommended by Seung Jin Song

The rotordynamic behavior of a hydraulic turbine is influenced by fluid-rotor interactions at the turbine runner. In this paper computational fluid dynamics (CFDs) are used to numerically predict the torsional dynamic coefficients due to added polar inertia, damping, and stiffness of a Kaplan turbine runner. The simulations are carried out for three operating conditions, one at about 35% load, one at about 60% load (near best efficiency), and one at about 70% load. The runner rotational speed is perturbed with a sinusoidal function with different frequencies in order to estimate the coefficients of added polar inertia and damping. It is shown that the added coefficients are dependent of the load and the oscillation frequency of the runner. This affect the system's eigenfrequencies and damping. The eigenfrequency is reduced with up to 65% compared to the eigenfrequency of the mechanical system without the fluid interaction. The contribution to the damping ratio varies between 30–80% depending on the load. Hence, it is important to consider these added coefficients while carrying out dynamic analysis of the mechanical system.

1. Introduction

Thomas [1] initiated the research on fluid-rotor interactions on turbines in 1958. He suggested an analytical model of destabilising forces due to nonsymmetric clearance in steam turbines. Alford [2] developed a similar model for compressors, where the forces are obtained as a function of the change in efficiency due to increased eccentricity. Urlichs [3] carried out the first research in a test rig and suggested corrections to Thomas and Alford's models. At the same time Iversen et al. [4], Agostinelli et al. [5], and Csanady [6] introduced models of hydraulic unbalance forces due to asymmetry of the flow channel geometry in centrifugal pumps. Hergt and Krieger [7] studied the influence of radial forces during off-design operating conditions. Colding-Jorgensen [8] used potential flow theory to determine damping and stiffness coefficients. Adkins [9] were the first to introduce an analytical model of both mass, damping and stiffness coefficients and harmonic forces. Adkins and Brennen [10], and Bolleter [11, 12] used test rigs to continue the development of models for fluid-rotor interactions of pump impellers. Childs [13] used bulk flow theory to determine rotordynamical coefficients at the pump-impeller-shroud surface.

The use of computational fluid dynamics (CFD) has recently increased within the area of fluid-rotor interactions. It was introduced by Dietzen and Nordmann [14] in 1987, but has due to the computational cost not been widely used in the past. The first applications of CFD within rotordynamics have been in the area of hydrodynamic bearings and seals. Recently, CFD has entered into the research of fluid-rotor interactions in centrifugal pumps [15]. CFD has been more common in research and development of hydraulic machinery. Ruprecht et al. [16, 17] used CFD to calculate forces and pressure pulsations on axial and Francis turbines. However, the results were not used in rotordynamical analysis. Liang et al. [18] carried out finite-element fluid-structure interactions of a turbine runner in still water and showed a reduction of the nonrotating eigenfrequencies compared to a runner in vacuum. The result had good agreement with the experimental results presented by Rodriguez et al. [19]. Karlsson et al. [20] analyzed the influence of different inlet boundary conditions on the resulting rotordynamic forces and moments for a hydraulic turbine runner. The benefits of using CFD to calculate rotordynamical forces and coefficients of hydraulic turbines have not yet been fully explored. In the present work CFD is used for the determination of the torsional dynamic coefficients due to the flow through the turbine.

2. Modelling and Simulation

2.1. Fluid-Dynamical Model

2.1.1. The OpenFOAM CFD Tool. In the present work the OpenFOAM (www.openfoam.org) open source CFD tool is used for the simulations of the fluid flow through the Hölleforsen water turbine runner. The simpleFoam OpenFOAM application is used as a base, which is a steady-state solver for incompressible and turbulent flow. It is a finite volume solver using the SIMPLE algorithm for pressure-velocity coupling. It has been validated for the flow in the Hölleforsen turbine by Nilsson [21]. New versions of the simpleFoam application have been developed in the present work, including Coriolis and centrifugal terms and unsteady RANS. All the computations use wall-function grids and turbulence is modelled using the standard $k - \epsilon$ turbulence model. The computations have been run in parallel on 12 CPUs on a Linux cluster, using the automatic decomposition methods in OpenFOAM. The version number used for the present computations is OpenFOAM 1.4.

2.1.2. Operating Conditions. All the computations are made for the Hölleforsen Kaplan turbine model runner, shown in Figure 1. The computational grid is obtained from earlier calculations by Nilsson [21]. The operating conditions used for the present investigations are for runner rotational speeds of 52 rad/s, 62 rad/s, and 72 rad/s, which correspond to loads of about 70%, 60%, and 35%, respectively. The boundary conditions are kept the same for all operating conditions (in the inertial frame of reference). The change in the load due to the rotational speed is explained by the fact that the pressure drop (or head of the system) needed to drive the same flow through the turbine will change with different rotational speed. The runner rotational speed is finally perturbed with a sinusoidal function in order to identify added coefficients for the torsional dynamic system. This is described below.

2.1.3. Boundary Conditions and Computational Grid. The inlet boundary condition was obtained by taking the circumferential average of a separate guide vane calculation, yielding an axisymmetric inlet flow [22]. This corresponds to a perfect distribution from the spiral casing and without any disturbance from the guide vane wakes.

Wall-functions and rotating wall velocities were used at the walls, and at the outlet the homogeneous Neumann boundary condition was used for all quantities. Recirculating flow was thus allowed at the outlet, and did occur. The turbulence quantities of the recirculating flow at the outlet are unknown, but to set a relevant turbulence level for the present case the back-flow values for k and ϵ were assumed to be similar to the average of those quantities at the inlet. The background of this assumption is that the turbulence level is high already at the inlet due to the wakes of the stay vanes and the guide vanes. It is thus assumed that the increase in turbulence level is small compared with that at the inlet. It is further believed that the chosen values are of minor importance for the overall flow. For the pressure the homogeneous Neumann boundary condition is used at all boundaries. The computations are made for a complete runner with five blades. The computational domain is shown by Figure 1 . A block-structured hexahedral wall-function grid was used, consisting of approximately 2 200 000 grid points.

Figure 1: The computational domain.

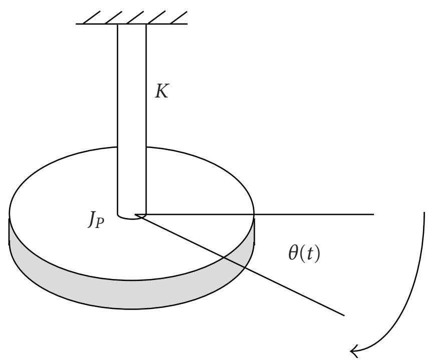

Figure 2: The mechanical model of a torsional dynamic system.

2.1.4. Discretization Schemes. For the convection divergence terms in the turbulence equations the Gamma discretization scheme by Jasak et al. [23] was used. For the convection divergence terms in the velocity equations the GammaV scheme was used, which is an improved version of the Gamma scheme formulated to take into account the direction of the flow field. The Gamma scheme is a smooth and bounded blend between the second-order central differencing (CD) scheme and the first-order upwind differencing (UD) scheme. CD is used wherever it satisfies the boundedness requirements, and wherever CD is unbounded UD is used. For numerical stability reasons, however, a smooth and continous blending between CD and UD is used as CD approaches unboundedness. The smooth transition between the CD and UD schemes is controlled by a blending coefficient β_m, which is chosen by the user. This coefficient should have a value in the range $0.2 \leq \beta_m \leq 1$, the smaller value the sharper switch and the larger value the smoother switch between the schemes. For good resolution, this value should theoretically be kept as low as possible, while higher values are more numerically stable. Studies of different β_m values have been made, and the results are however more or less unaffected by the choice of β_m. In the present work a value of $\beta_m = 1.0$ has been used. The time derivative is discretized using the Euler implicit method.

2.2. Identification of Dynamic Coefficients. To describe how the eigenfrequencies and damping of a torsional dynamic system change due to the flow, the model illustrated in Figure 2 is used. In the model, the generator is assumed to be stiff due to the connection to a rigid electric grid, and hence only the torsional motion of the turbine runner is considered. The equation of motion for this system is given by

$$J_P\ddot{\theta} + C\dot{\theta} + K\theta = M(t), \tag{1}$$

where J_P is the polar inertia, C is the damping, K is the stiffness, $M(t)$ an external moment, t is the time, θ is the angular displacement, $\dot{\theta}$ is the angular velocity, and $\ddot{\theta}$ is the angular acceleration. It is further assumed that the flow through a turbine will give additional inertia, damping, and stiffness to the system. With these additional coefficients the equation of motion becomes

$$(J_P + J_{P,\text{Fluid}})\ddot{\theta} + (C + C_{\text{Fluid}})\dot{\theta} + (K + K_{\text{Fluid}})\theta = M(t), \tag{2}$$

where $J_{P,\text{Fluid}}$ is the added polar inertia, C_{Fluid} is the added damping, and K_{Fluid} is the added stiffness. External moments are negligible ($M(t) = 0$) in the present work. CFD is used to identify the added coefficients from the torque of the turbine runner. Rewriting the moments due to the flow to

$$T'(t) = -J_{P,\text{Fluid}}\ddot{\theta} - C_{\text{Fluid}}\dot{\theta} - K_{\text{Fluid}}\theta, \tag{3}$$

where $T'(t)$ is the total torsional moment due to the flow, and inserting this into (2) yields

$$J_P\ddot{\theta} + C\dot{\theta} + K\theta = T'(t). \tag{4}$$

To solve $T'(t)$, the forces and moments from the CFD-simulations are calculated at each time step. The force on a control volume boundary face is given by

$$\vec{F}_{\text{face},i} = p_{\text{face},i}A_{\text{face},i}\vec{n}_{\text{face},i}, \tag{5}$$

where $p_{\text{face},i}$ is the pressure of the face, $A_{\text{face},i}$ is the area of the face, and $\vec{n}_{\text{face},i}$ is the normal vector of the face. The moment of the centre of gravity of the runner at a face is

$$\vec{M}_{\text{face},i} = \vec{F}_{\text{face},i}r_{\text{face},i}, \tag{6}$$

where r_{face} is the radius from the centre of gravity to the face. The total moment is calculated as

$$\vec{M} = \sum_{i=1}^{n}\vec{M}_{\text{face},i}, \tag{7}$$

where n is the number of faces. The torque is obtained as a scalar product of the moment and the direction vector of the shaft

$$T(t) = \vec{M}\vec{n}_y. \tag{8}$$

During steady conditions the torque is constant in order to provide a constant power to the generator. In case of unsteady conditions, the torque can be written as

$$T(t) = T_{\text{mean}} + T'(t), \tag{9}$$

where T_{mean} is the constant part of the torque. In the present work the rotational speed of the turbine runner is prescribed in order to determine the dynamical coefficients of the turbine runner due to the flow. The angular displacement of the runner is given by

$$\theta = \Omega t + a\cos(\vartheta t) = \Omega t + \theta', \tag{10}$$

where Ω is the constant angular velocity, t is the time, a is an amplitude, ϑ is a frequency of the prescribed runner oscillation, and θ' is the oscillating part of θ. Below, we are only interested in the oscillating part, where

$$\theta' = a\cos(\vartheta t), \tag{11}$$

gives the velocity

$$\dot{\theta}' = -a\vartheta\sin(\vartheta t), \tag{12}$$

and the acceleration

$$\ddot{\theta}' = -a\vartheta^2\sin(\vartheta t). \tag{13}$$

Inserting (11), (12), and (13) into (3) results in an equation for the fluctuation of the torque

$$T'(t) = a\vartheta^2 J_{P,\text{Fluid}}\cos(\vartheta t) + a\vartheta C_{\text{Fluid}}\sin(\vartheta t) - aK_{\text{Fluid}}\cos(\vartheta t). \tag{14}$$

This can be written as

$$T'(t) = T_{\text{Amp}}\cos(\vartheta t - \phi) = T_1\cos(\vartheta t) + T_2\sin(\vartheta t), \tag{15}$$

where T_{Amp} is the amplitude of the torque, ϕ is the phase angle, and T_1 and T_2 are the cosine and sine components of the amplitude. Then the additional damping due to the fluid can be identified as

$$C_{\text{Fluid}} = \frac{T_2}{a\vartheta}, \tag{16}$$

and the additional stiffness and polar inertia due to the fluid can be identified by solving

$$a\vartheta^2 J_{P,\text{Fluid}} - aK_{\text{Fluid}} = T_1 \tag{17}$$

for two simulations with different values of ϑ.

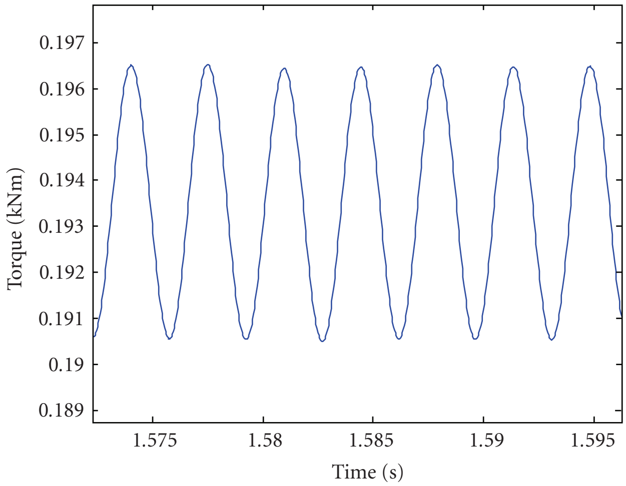

FIGURE 3: The torque as a function of time for one of the simulated cases (rotational speed is 72 rad/s and the oscillating frequency is 1809 rad/s).

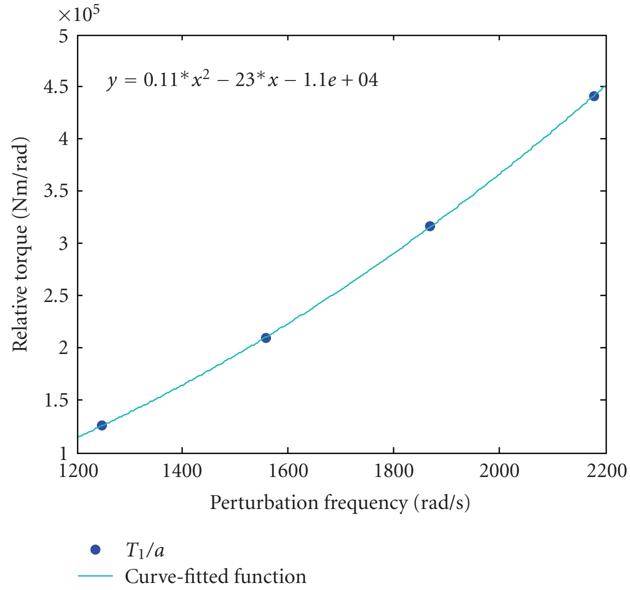

FIGURE 4: Identification of the coefficients of (17), together with a curve-fitted function (rotational speed is 52 rad/s).

The eigenfrequency of (2) can now be solved as

$$\omega_D = \sqrt{\frac{K + K_{\text{Fluid}}}{J_P + J_{P,\text{Fluid}}} - \frac{(C + C_{\text{Fluid}})^2}{4(J_P + J_{P,\text{Fluid}})^2}}, \tag{18}$$

and the corresponding damping ratio is

$$\zeta = \frac{C + C_{\text{Fluid}}}{2(J_P + J_{P,\text{Fluid}})\sqrt{(K + K_{\text{Fluid}})/(J_P + J_{P,\text{Fluid}})}}. \tag{19}$$

3. Results

In Figure 3 the torque is shown as a function of time for one of the simulated cases. The amplitude of T_1/a in (17) is presented as a function of perturbation frequency in Figure 4. The perturbation amplitude is $a = 4.0 \times 10^{-6}$ rad for all simulations and is selected in the area where torque/angular velocity is linear and the value is selected in order to separate the response from numerical noise. One can see that it is difficult to identify the coefficients as stated in (17). There are two possible explanations to this: the coefficients depend on frequency and the stiffness is probably small due to the incompressible fluid. The stiffness is therefore assumed to be negligible ($K_{\text{Fluid}} = 0$ in (17)) in the analysis below. The added polar inertia is presented in Figure 5 and the added damping in Figure 6.

The later coefficients are added to the mechanical system, that is, (2). The polar inertia of the mechanical system is $J_P = 1.57\,\text{Nms}^2$, the damping is $C = 0$ Nms, and the stiffness is $K = 49000$ Nm. In Figure 7 the reduced eigenfrequencies (18) and in Figure 8 the damping ratio (19) due to the flow for such a fluid-mechanical system are presented and the influence of the different coefficients is illustrated.

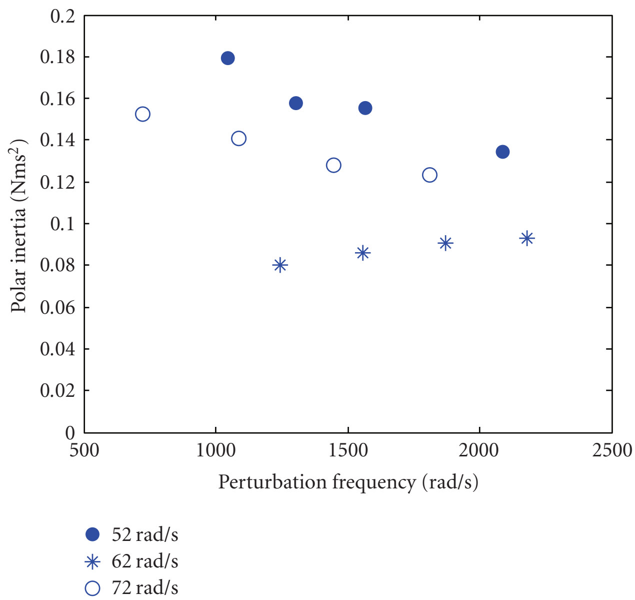

FIGURE 5: Additional polar inertia as a function of perturbing frequency and operating condition.

4. Discussion

Both added polar inertia and damping have a significant effect on the eigenfrequency of the mechanical system. The added polar inertia decreases the eigenfrequency 3–5% for all cases (see Figure 7). Concerning the damping, an additionally decrease of the eigenfrequency of 5–60% is observed (see Figure 7). One can see that both damping and polar inertia increases for off-nominal speed and with frequency. Recent research by Liang et al. [18], and Rodriguez et al. [19] has

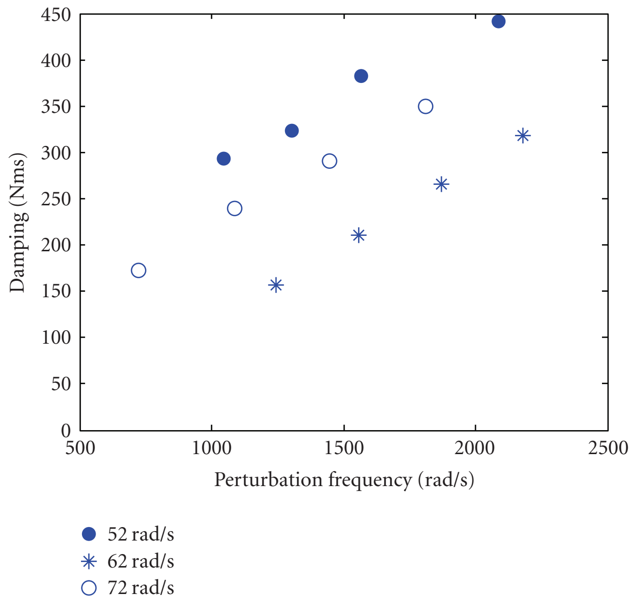

Figure 6: Additional damping as a function of perturbing frequency and operating condition.

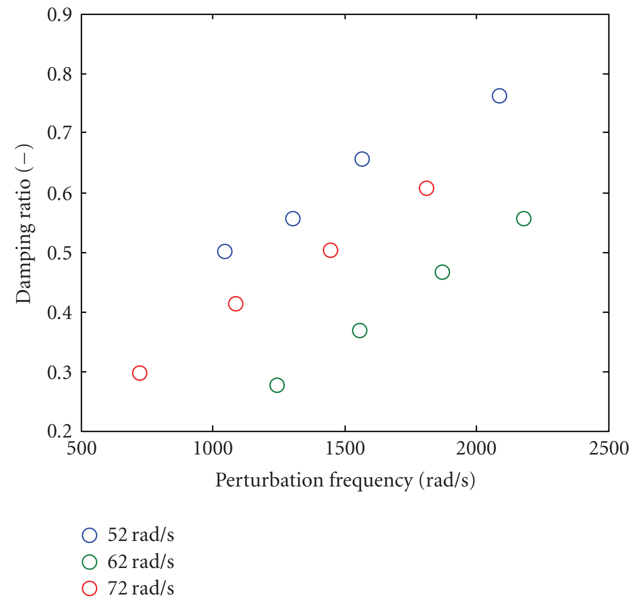

Figure 8: Additional damping due to the flow through the turbine (the damping of the mechanical system is zero).

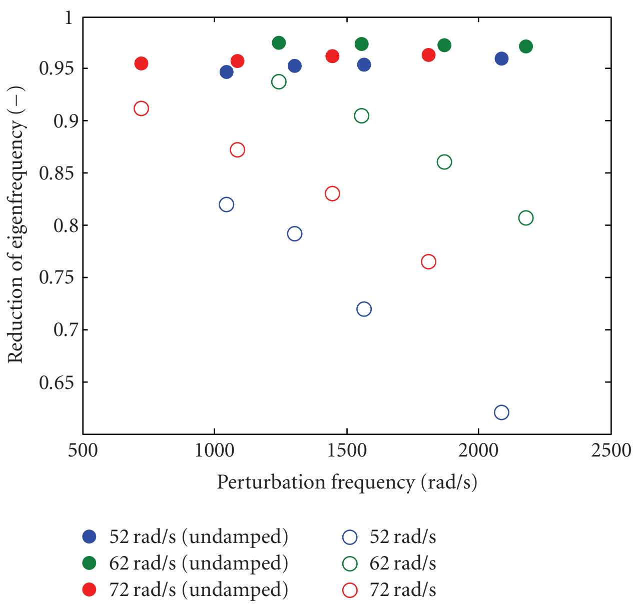

Figure 7: Reduction of the eigenfrequency (the eigenfrequency of the mechanical system is 1) due to the flow through the turbine. The "undamped" markers represent the effect of an added polar inertia alone.

shown that the eigenfrequencies are reduced by 10–39% for a nonrotating Francis runner in still water. The effect of added inertia in these papers are significantly higher than the case of nominal operating condition in the present work and the authors observe no strong effect of damping. An explanation to the difference between the present study and the earlier work is the dependency of frequency for both added inertia and damping and that the present work includes the turbine flow.

Iso-surfaces are here used to illustrate the difference between the different operating conditions. Figure 9 shows iso-surfaces of regions where the turbulent kinetic energy is high. In Figures 10, 11, and 12 smearlines at the blades are presented in order to see the details of the flow.

The difference in the rotating speed results in different flow conditions for the different operating conditions. The guide vane angle is equal for all cases. Hence, the angle of attack at the leading edge of the runner blades is changed when changing the rotational speed. The tipclearance flow from the pressure side to the suction side is increased when the rotational speed is reduced. For high rotational speeds there is also a tip vortex at the runner blade pressure side due to the unfavorable angle of attack close to the tip. The tip vortex flow is the reason to the high turbulent kinetic energy near the tipclearence, which is shown in Figure 9. Figure 9 also shows high turbulence kinetic energy in the flow stagnation at the leading edges of the runner blades, and in separation regions. A major difference in the level of turbulence kinetic energy can be found below the runner cone in the recirculation region. The significant differences of the flow field for the different cases are also illustrated by the smearlines in Figures 10, 11, and 12. Figures 10 and 12 show a large non-axisymmetric recirculation area below the cone. The wakes below the runner vanes are also shown on the cone as well as the tipvortex flow. Figure 11 shows a small axisymmetric recirculation area below the cone.

Recent research of added mass of a cylinder by Wang et al. [24] has shown that the added mass is dependent on the velocity around a cylinder. The same effect is suspected in the present study, where the flow velocity differs between the cases.

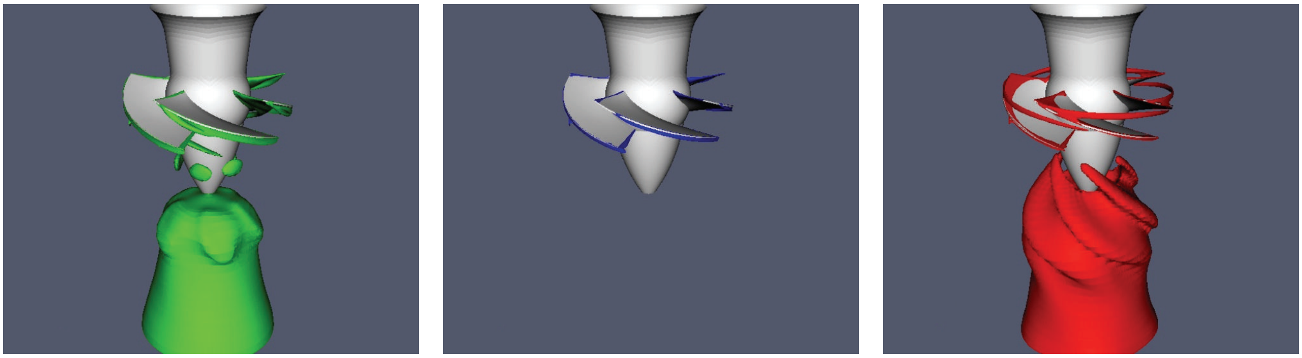

(a) (b) (c)

Figure 9: Iso-surface of turbulent kinetic energy, (a) 52 rad/s, (b) 62 rad/s, and (c) 72 rad/s.

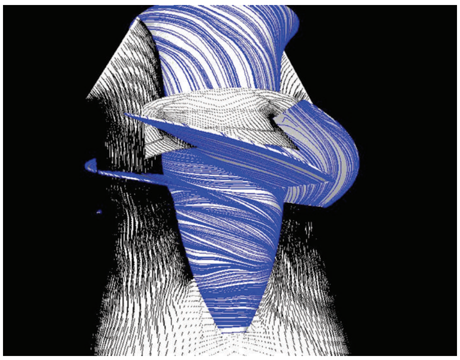

Figure 10: Smearlines and velocity vectors for 52 rad/s.

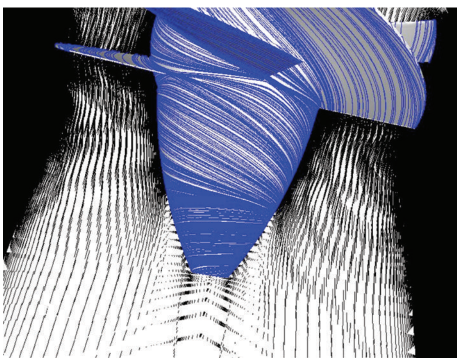

Figure 11: Smearlines and velocity vectors for 62 rad/s.

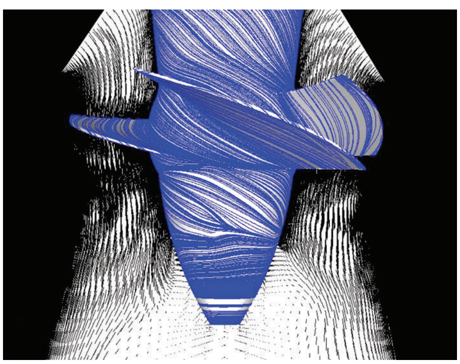

Figure 12: Smearlines and velocity vectors for 72 rad/s.

5. Conclusions

The added polar inertia and damping due to the hydraulic system significantly affect the mechanical system. This results in a reduced eigenfrequency of 5–65% and an increase in the damping of 30–80%. It is further concluded that the added coefficients are dependent on the turbine load and oscillating frequency. A change in the system properties of the mechanical system is important to consider in design and operation. Future studies should include experimental verification of the results in the present work.

Nomenclature

θ: Angular displacement (rad)
ω_D: Damped natural frequency (rad/s)
ζ: Damping ratio (−)
ϑ: Prescribed frequency (rad/s)
Ω: Rotational speed (rad/s)
$\vec{n}_{\text{face},i}$: Normal vector at one face (−)
$p_{\text{face},i}$: Pressure one face (N/m^2)
t: Time (s)
$A_{\text{face},i}$: Area of one face (Nm)
C: Damping (Nms/rad)
C_{Fluid}: Added damping (Nms/rad)
$\vec{F}_{\text{face},i}$: Force on one face (N)
J_P: Polar moment of inertia (kgm^2)
$J_{P,\text{Fluid}}$: Added Polar moment of inertia (kgm^2)
K: Stiffness (Nm/rad)
K_{Fluid}: Added stiffness (Nm/rad)
$M(t)$: External moment (Nm)
$\vec{M}_{\text{face},i}$: Moment at one face (Nm)
$T'(t)$: Total torsional torque due to flow (Nm)
$T_{1,2}$: Sine and cosine components of the torque (Nm)
T_{Amp}: Amplitude of the oscillating part of the torque (Nm)
T_{Mean}: Constant part of the torque (Nm)

Acknowledgments

The research presented in this paper has been carried out with funding by Elforsk AB and the Swedish Energy Agency through their joint Elektra programme and as a part of the Swedish Hydropower Centre (SVC) (http://www.svc.nu/). SVC has been established by the Swedish Energy Agency, Elforsk, and Svenska Kraftnät together with Luleå University of Technology, The Royal Institute of Technology, Chalmers University of Technology, and Uppsala University. Computations have been carried out with support from the Swedish National Infrastructure for Computing on the Hive and Ada clusters at C3SE, Chalmers University of Technology.

References

[1] J. J. Thomas, "Instabile Eigenschwingungen von Turbinenlaufen, Angefacht durch die Spaltstromnungen in Stopfbuchen und Beschau ungen," *AEG-Sonderdruck*, pp. 1039–1063, 1958.

[2] J. S. Alford, "Protection turbomachinery from self-excited rotor whirl," *Journal of Engineering for Power*, pp. 333–335, 1965.

[3] K. Urlichs, "Leakage flow in thermal turbo-machines as the origin of vibration-exciting lateral forces," Tech. Rep. NASA TT-17409, NASA, Washington, DC, USA, March 1977.

[4] H. W. Iversen, R. E. Rolling, and J. J. Carlson, "Volute pressure distribution, radial forces on the impeller and volute mixing losses of a radial flow centrifugal pump," *ASME Journal of Engingeering for Power*, vol. 82, pp. 136–144, 1960.

[5] A. Agostinelli, D. Nobles, and C. R. Mockridge, "An experimental investigation of radial thrust in centrifugals pumps," *ASME Journal of Engineering for Power*, vol. 82, pp. 120–126, 1960.

[6] G. T. Csanady, "Radial forces in a pump caused by volute casing," *ASME Journal of Engineering for Power*, vol. 84, pp. 337–340, 1962.

[7] P. Hergt and P. Krieger, "Radial forces in centrifugal pumps with guide vanes," *Proceedings of the Institution of Mechanical Engineers*, vol. 184, part 3N, pp. 101–107, 1969-1970.

[8] J. Colding-Jorgensen, "The effect of fluid forces on rotor stability of centrifugal compressors and pumps," in *Proceedings of the 1st Workshop on Rotordynamic Instability Problems in High-Performance Turbomachinery*, pp. 249–266, Texas A&M University, College Station, Tex, USA, May 1980, NASA Conference Publication no. 2443.

[9] D. R. Adkins, *Analysis of hydrodynamic forces on centrifugal pump impellers*, Ph.D. thesis, California Institute of Technology, Pasadena, Calif, USA, 1985.

[10] D. R. Adkins and C. E. Brennen, "Analysis of hydrodynamic radial forces on centrifugal pump impellers," *ASME Journal of Fluid Engingeering*, vol. 110, pp. 20–28, 1988.

[11] U. Bolleter, A. Wyss, I. Welte, and R. Stürchler, "Measurement of hydrodynamic interaction matrices of boiler feed pump impellers," *Journal of Vibration, Acoustics, Stress, and Reliability in Design*, vol. 109, no. 2, pp. 144–151, 1987.

[12] U. Bolleter, E. Leibundgut, R. Stürchler, and T. McCloskey, "Hydraulic interaction and excitation forces of high head pump impellers," in *Proceedings of the 3rd Joint ASCE/ASME Mechanics Conference*, vol. 81, pp. 187–193, UCSD, San Diego, Calif, USA, July 1989.

[13] D. W. Childs, "Fluid-structure interaction forces at pump-impeller-shroud surfaces for rotordynamic calculations," *Journal of Vibration, Acoustics, Stress, and Reliability in Design*, vol. 111, no. 3, pp. 216–225, 1989.

[14] F. J. Dietzen and R. Nordmann, "Calculating rotordynamic coefficients of seals by finite-difference techniques," *Journal of Tribology*, vol. 109, no. 3, pp. 388–394, 1987.

[15] T. Suzuki, K. Yonezawa, H. Horiguchi, T. Tsukiya, Y. Taenaka, and Y. Tsjuimoto, "A numerical analysis of rotordynamic uid forces on an artificial heart pump impeller in whirling motion," in *Proceedings of the 12th International Symposium on Transport Phenomena and Dynamics of Rotating Machinery*, Honolulu, Hawaii, USA, February 2008, paper-ID ISROMAC12-2008-20232.

[16] A. Ruprecht, C. Bauer, and M. Heitele, "Unsteady forces on the blading of an axial turbine caused by stator-rotor interaction," in *Proceedings of the 9th IAHR WG International Meeting on the Behavior of Hydraulic Machinery under Steady Oscillatory Conditions*, Brno, Czech Republic, September 1999.

[17] A. Ruprecht, M. Heitele, T. Helmrich, W. Moser, and T. Aschenbrenner, "Numerical simulation of a complete francis turbine including unsteady rotor/stator interactions," in *Proceedings of the 20th IAHR Symposium on Hydraulic Machinery and Systems*, pp. 1–8, Charlotte, NC, USA, August 2000.

[18] Q. W. Liang, C. G. Rodriguez, E. Egusquiza, X. Escaler, M. Farhat, and F. Avellan, "Numerical simulation of uid added mass effect on a francis turbine runner," *Computers & Fluids*, vol. 36, pp. 1106–1118, 2007.

[19] C. G. Rodriguez, E. Egusquiza, X. Escaler, Q. W. Liang, and F. Avellan, "Experimental investigation of added mass effects on a Francis turbine runner in still water," *Journal of Fluids and Structures*, vol. 22, no. 5, pp. 699–712, 2006.

[20] M. Karlsson, H. Nilsson, and J.-O. Aidanpää, "Influence of inlet boundary conditions in the predictions of rotor dynamic forces and moments for a hydraulic turbine using CFD," in *Proceedings of the 12th International Symposium on Transport Phenomena and Dynamics of Rotating Machinery*, Honolulu, Hawaii, USA, February 2008, paper-ID ISROMAC12-2008-20078.

[21] H. Nilsson, "Evaluation of OpenFOAM for CFD of turbulent flow in water turbines," in *Proceedings of the 23rd IAHR Symposium on Hydraulic Machinery and Systems*, Yokohama, Japan, October 2006.

[22] H. Nilsson and L. Davidson, "A numerical investigation of the flow in the Wicket gate and runner of the Hölleforsen (Turbine-99) Kaplan turbine model," in *Proceedings of the Turbine-99—Workshop 2: The 2nd ERCOFTAC Workshop on Draft Tube Flow*, Älvkarleby, Sweden, June 2001.

[23] H. Jasak, H. G. Weller, and A. D. Gosman, "High resolution nvd differencing scheme for arbitrarily unstructured meshes," *International Journal for Numerical Methods in Fluids*, vol. 31, no. 2, pp. 431–449, 1999.

[24] Y. Wang, W. Chen, and M. Lin, "Variation of added mass and its application to the calculation amplitude response for a circular cylinder," *China Ocean Engineering*, vol. 21, no. 3, pp. 429–437, 2007.

Advances in Mechanical Engineering

Special Issue on Micro/Nanotransport Phenomena in Renewable Energy and Energy Efficiency

Call for Papers

Energy has become one of the most important issues of our time as a result of serious concerns about climate change, high oil prices, and peak oil. Renewable energy and energy-saving technologies are potentially crucial parts of the ultimate solutions to both energy sustainability and climate change. Although there are plenty of renewable energy sources available, such as solar, wind, geothermal, they each have some drawbacks: being intermittent, low efficiency and high capital cost, which, at present, limits their applicability. Micro- and nanoscale transport phenomena can play critical role in developing technologies to supply clean energy with both low cost and high efficiency. For example, thermoelectric materials (TE) have application in waste heat recovery and solar energy as well as in the construction of compact coolers or even AC if TE merit, or ZT, can reach 3 or higher. However, it is very challenging to create a perfect TE material with easy electron passage and low phonon flow resistance at the same time. Most recently, nanoscale thermoelectric materials with ZTs as high as 1.4 have been reported, which translates to an efficiency of 14%. Another example is the possibility of using sunlight to breakdown water into hydrogen and oxygen by mimicking photosynthesis. To enable efficient artificial photosynthesis, it is necessary to make artificial multiple electron systems. A breakthrough has been made to accept multiple electrons and release them from single-walled carbon nanotubes (SWNTs) and Phthalocyanines (PCs). Using a catalyst is yet another way to make hydrogen gas from water. A cheap inorganic catalyst has been developed to effectively split hydrogen from water by using sunlight. Additionally, the advanced micro- and nanoscale surface treatment technologies and structures are also very important to the improvement of renewable energy producing and end use efficiencies. Advances in micro- and nanoscale transports can play a crucial role in exploiting renewable energy and developing energy saving technologies in the future. These technologies hold the possibility of providing groundbreaking increases in renewable energy process yields, efficiencies, and lower overall costs, but there is still much to be done before industrializing these technologies. This special issue focuses on these challenges and solicits papers in relevant areas, including, but not limited to, the following:

- Particle transport phenomena in renewable energy conversion processes
- Micro/nanoscale engineered materials for energy conversion and storage
- Fluid transport in micro/nanoscale structures for energy producing process and end use
- Multiphysical transport in microporous media
- Systematical optimization of energy efficiency

Before submission authors should carefully read over the journal's Author Guidelines, which are located at http://www.hindawi.com/journals/ame/guidelines.html. Authors should follow the Advances in Mechanical Engineering manuscript format described at the journal site http://www.hindawi.com/journals/ame/. Prospective authors should submit an electronic copy of their complete manuscript through the journal Manuscript Tracking System at http://mts.hindawi.com/ according to the following timetable:

Manuscript Due	July 1, 2009
First Round of Reviews	October 1, 2009
Publication Date	January 1, 2010

Lead Guest Editor

G. P. "Bud" Peterson, Office of the President, 225 North Avenue, NW, Atlanta, GA 30332-0325, USA; bud.peterson@gatech.edu

Guest Editors

Gang Chen, Department of Mechanical Engineering, Massachusetts Institute of Technology, MA 02139, USA; gchen2@mit.edu

Moran Wang, Los Alamos National Laboratory, Los Alamos, NM 87545, USA; mwang@lanl.gov

Chen Li, Department of Mechanical Engineering, University of Colorado, Boulder, CO 80309, USA; lichen.cu@colorado.edu

Special Issue on Computational Stochastic Structural Dynamics

Call for Papers

For safety and reliability reasons, many dynamic engineering systems excited by intensive forces with irregular time histories have to be analyzed and designed by employing statistical concepts. The development of jet and rocket propulsion systems in the 1940's and subsequently the development of commercial jet aeroplanes in the 1950's that introduced a problem of structural vibration are a good example. In the middle of 1950's and early 1960's, the accelerated development of computers and computational techniques, such as the finite-element method, has enabled the designers to provide less conservative designs for more sophisticated and complex structural systems. Since the early 1950's, many national and international conferences as well as symposia have partially or entirely devoted to presenting results in the field of computational stochastic structural dynamics. It is believed that the latter has reached a stage in which a detailed comparison of the various classes of computational techniques and an examination of design issues for large-scale structural systems are warranted.

The goal of this Special Issue is, therefore, to solicit and publish the most recent research and development in the field, with particular focus on applications of various classes of computational techniques, and to design issues of existing as well as future structural dynamic engineering systems.

Topics of interest include, while strictly confined to the field of computational stochastic structural dynamics, but are not limited to:

- Linear mechanical and structural systems under random excitations
- Nonlinear mechanical and structural systems in aerospace, offshore and ocean, earthquake, automotive, bridge, railway and tunnel, and nuclear engineering
- Future mechanical and structural systems in random environments

Before submission, authors should carefully read over the journal's Author Guidelines, which are located at http://www.hindawi.com/journals/ame/guidelines.html. Prospective authors should submit an electronic copy of their complete manuscript through the journal Manuscript Tracking System at http://mts.hindawi.com/, according to the following timetable:

Manuscript Due	August 1, 2009
First Round of Reviews	November 1, 2009
Publication Date	February 1, 2010

Lead Guest Editor

Cho W. Solomon To, Department of Mechanical Engineering, University of Nebraska, N104 Scott Engineering Center, Lincoln, NE 68588, USA; cto2@unl.edu

Guest Editors

Solomon C. Yim, School of Civil and Construction Engineering, Oregon State University, 220 Owen Hall, Corvallis, OR 97331, USA; solomon.yim@oregonstate.edu

Brian Mace, Institute of Sound and Vibration Research, University of Southampton, Southampton SO17 1BJ, UK; brm@isvr.soton.ac.uk

Special Issue on Heat Transfer in Nanofluids

Call for Papers

Heat transfer can be enhanced by employing various techniques and methodologies, such as increasing either the heat transfer surface or the heat transfer coefficient between the fluid and the surface, which allow high heat transfer rates in a small volume. Cooling is one of the most important technical challenges facing many diverse industries, including microelectronics, transportation, solid-state lighting, and manufacturing.

There is, therefore, an urgent need for new and innovative coolants with improved performance. The novel concept of "nanofluids" has been proposed as a route to surpassing the performance of heat transfer fluids currently available. Several investigations have revealed that the thermal conductivity of the fluid containing nanoparticles could be increased by more than 20% for the case of very low nanoparticle concentrations. Nowadays, a fast growth of research activity in this heat transfer area has arisen.

The aim of this special issue is to collect original research articles as well as review articles on the most recent developments and research efforts in this field, with the purpose of providing guidelines for future research directions.

Topics of interest include, but are not limited to:

- Experimental techniques for measuring thermal properties of nanofluids
- Single-phase convection
- Natural and forced convection cooling
- Pool and flow boiling applications
- Nucleate boiling and critical heat flux and post-CHF measurements
- Flow and heat transfer characteristics in the laminar and turbulent regimes
- Modeling of flow and heat transfer behavior of nanoparticles, nanotubes, and nanofluids under equilibrium and nonequilibrium conditions
- Applications including cooling of electronics, vehicles, fuel cells, transformers, nuclear systems, space systems, drilling, lubrication, thermal storage, drag reduction, and biomedical applications

Before submission authors should carefully read over the journal's Author Guidelines, which are located at http://www.hindawi.com/journals/ame/guidelines.html. Authors should follow the Advances in Mechanical Engineering manuscript format described at the journal site http://www.hindawi.com/journals/ame/. Prospective authors should submit an electronic copy of their complete manuscript through the journal Manuscript Tracking System at http://mts.hindawi.com/ according to the following timetable:

Manuscript Due	July 1, 2009
First Round of Reviews	October 1, 2009
Publication Date	January 1, 2010

Lead Guest Editor

Oronzio Manca, Dipartimento di Ingegneria Aerospaziale e Meccanica, Seconda Università degli Studi di Napoli, Viale Beneduce 10, Via Roma 29, Aversa (CE) 81031, Italy; oronzio.manca@unina2.it

Guest Editors

Yogesh Jaluria, School of Engineering, Rutgers, The State University of New Jersey, 98 Brett Road, Piscataway, NJ 08854-8058, USA; jaluria@jove.rutgers.edu

Dimos Poulikakos, Laboratory of Thermodynamics in Emerging Technologies, Institute of Energy Technology, Swiss Federal Institute of Technology, 8092 Zurich, Switzerland; dimos.poulikakos@ethz.ch